Acceleration waves in a spherical oscillating gas bubble containing a gas mixture

Acceleration waves in a spherical oscillating gas bubble containing a gas mixture

Francesca Brini[1*] and Leonardo Seccia[2†]

[1*]Department of Mathematics, University of Bologna, via Saragozza, 8, Bologna, I-40123, Italy.
[2]Department of Mathematics, University of Bologna, via Fontanelle, 40, Forlì, I-47121, Italy.

*Corresponding author(s). E-mail(s): francesca.brini@unibo.it;
Contributing authors: leonardo.seccia@unibo.it;
†These authors contributed equally to this work.

Abstract

The non-equilibrium phenomena that characterize the dynamics of an oscillating bubble in a liquid are generally very complex. In this work we study the effects produced by the presence of a gas mixture in which the temperatures of each species are taken into account. Acceleration waves are used to test the stabilizing effects of the model and verify the possibility of shock formation within the bubble. It is shown that the diffusion associated with the presence of multiple temperatures cannot be neglected when describing what happens inside the bubble, even in the sonoluminescence regime.

Keywords: Oscillating gas bubble, Acceleration wave, Euler gas, Multi-temperature gas mixture

1 Introduction

The dynamics of gas bubbles oscillating in a liquid in the presence of a periodic acoustic signal is a complex and fascinating topic that brings together different aspects of physics and mathematics. It currently attracts a lot of attention given the enormous number of applications in medicine, engineering, chemistry, etc. Consequently, the literature on this subject is very extensive and we will only mention a few review

works here [1–5], but many features (such as the gas dynamics inside the bubble) still remain not entirely clear.

In particular, the behaviour of a gas enclosed in an oscillating bubble has often been studied in the framework of an Euler gas, thus neglecting its thermal conductivity and viscosity, while maintaining the hyperbolic structure of the balance laws. Under these conditions of absence of dissipation, the possible formation of a shock inside the bubble has been predicted as accompanying the observation of a flash of light in the sonoluminescence regime (SL) [6–8]. In a previous work [9] we have already shown that the dissipation associated to viscosity and thermal conductivity strongly inhibits the shock formation, as suggested by several authors by means of different techniques [4, 10, 11]. In [9], as in the present work, the verification was conducted through the analysis of the acceleration wave behaviour. Acceleration waves (AW), also called weak discontinuity or C^1 discontinuity waves, are propagating surfaces representing a particular solution of a PDE's system. As a matter of fact, its field variables are continuous everywhere, but their first order spatial derivatives can have a discontinuity jump across the surface. AWs have been studied in different frameworks and here we quote some works and applications in the case of gases [6, 9, 12–23].

While in the past we introduced rational extended thermodynamic models to describe the phenomena involving heat conductivity and viscosity [9], now we focus on the dissipation effects related to the presence of a multi-temperature gas mixture. Usually a gas mixture, such as air, inside the bubble is modelled as a single gas with average physical constants [7, 8]. The idea of focusing on a multi-temperature mixture of Euler (MT) gases is related to the fact that the relaxation time associated with the multiple temperatures could be longer than that of thermal conductivity or viscosity. The effect we are about to describe is observable even when the molecular masses of the components are equal, provided that they have different ratios of specific heats. Hence, for instance, the simultaneous presence of monatomic and polyatomic gases in the bubble could stabilize the bubble dynamics, including when heat conductivity is neglected.

The paper is organized as follows. The AW theory is briefly presented in Sec. 2, while Sec. 3 summarizes a simplified model of bubble oscillation and the qualitative description of SL regime. The Euler gas mixture model with multi-temperature is introduced in Sec. 4. Sec. 5 contains the analytical and numerical results together with some remarks. Finally, the conclusions can be found in Sec. 6.

2 Acceleration wave theory

Let us consider a surface Γ that propagates in space. In front of the wavefront the unperturbed field variables are known functions $\mathbf{u}_u(\mathbf{z}, t)$ of space $\mathbf{z}$ and time t, while behind the wavefront the perturbed field variables are usually unknown. This surface represents an acceleration wave if the discontinuity of the derivative of one or more field variables occurs through it, while the field variables, $\mathbf{u}$, themselves remain continuous. The previous conditions could be written as $[\![\mathbf{u}]\!] = 0$ and $[\![\frac{\partial \mathbf{u}}{\partial \phi}]\!] = \boldsymbol{\mathcal{A}} \neq \mathbf{0}$, if $\phi(\mathbf{z}, t) = 0$ is the equation of the wavefront and $[\![\,\cdot\,]\!] = (\cdot)_{\phi=0^-} - (\cdot)_{\phi=0^+}$ represents the jump across Γ. In this work we focus on spherical AWs travelling in the radial direction, so

that by introducing spherical coordinates we deal with a one-dimensional phenomenon, for which the AW theory predicts that [12, 15, 16]:

- The normal velocity $V = -\phi_t/|\nabla\phi|$ of the wave front coincides with the characteristic speed of the hyperbolic PDE system evaluated in the unperturbed field $V = \lambda(\mathbf{u}_u)$.
- The jump vector $\boldsymbol{\mathcal{A}}$ is proportional to the right eigenvectors corresponding to λ, evaluated in $\mathbf{u}_u$, so that $\boldsymbol{\mathcal{A}} = \mathcal{A}\mathbf{r}(\mathbf{u}_u)$.
- The scalar amplitude $\mathcal{A}$ satisfies the Bernoulli equation

$$\frac{d\mathcal{A}}{dt} + a(t)\mathcal{A}^2 + b(t)\mathcal{A} = 0, \tag{1}$$

  if d/dt indicates the time derivative along the characteristic line ($dx/dt = \lambda(\mathbf{u}_u)$) and $a(t)$ and $b(t)$ are suitable functions of time.

From equation (1), the scalar amplitude of the jump is easily obtained as a function of time by prescribing its initial value $\mathcal{A}(t=0) = \mathcal{A}_0$:

$$\mathcal{A}(t) = \frac{\mathcal{A}_0 g_1(t)}{1 + \mathcal{A}_0 g_2(t)} \quad \text{with } g_1(t) = \exp\left(-\int_0^t b(s)ds\right) \quad \text{and} \quad g_2(t) = \int_0^t a(s)g_1(s)ds. \tag{2}$$

Concerning the calculation of the Bernoulli's coefficients a and b, for one-dimensional waves and for a set of PDEs written as

$$\partial_t \mathbf{u} + \mathbf{A}(\mathbf{u}, z, t)\partial_z \mathbf{u} = \mathbf{T}(\mathbf{u}, z, t), \tag{3}$$

it was shown that [16]

$$\begin{aligned} a(t) &= \phi_z(t)(\nabla_{\mathbf{u}}\lambda \cdot \mathbf{r})\Big|_u, \\ b(t) &= \left\{\mathbf{r}((\nabla_{\mathbf{u}}\mathbf{l})^T - \nabla_{\mathbf{u}}\mathbf{l}) \cdot \frac{d\mathbf{u}}{dt} + (\nabla_{\mathbf{u}}\lambda \cdot \mathbf{r})(\mathbf{l} \cdot \mathbf{u}_z) - \nabla_{\mathbf{u}}(\mathbf{l} \cdot \mathbf{T}) \cdot \mathbf{r} + \mathbf{l} \cdot \frac{\tilde{d}\mathbf{r}}{dt}\right\}\Big|_u, \end{aligned} \tag{4}$$

if $w_z = \partial w/\partial z$ for any w and $\nabla_{\mathbf{u}}\cdot = \partial\cdot/\partial\mathbf{u}$. In addition, $\mathbf{l}(\mathbf{u}, z, t)$ and $\mathbf{r}(\mathbf{u}, z, t)$ denote respectively the left and right eigenvector of $\mathbf{A}$ associated with the eigenvalue λ. For any function w of the field variables we refer to the notation: $w|_u = w(\mathbf{u}_u)$, while $\frac{d\cdot}{dt} = \partial_t\cdot + \lambda_u\partial_z\cdot$ and $\frac{\tilde{d}\cdot}{dt} = (\frac{d\cdot}{dt})|_{\mathbf{u}=const}$. The left and right eigenvectors are prescribed according to [9, 22], so that the scalar amplitude coincides with the acceleration jump $\mathcal{G} = \left[\!\left[\frac{\partial v}{\partial t}\right]\!\right] = -\lambda_u\left[\!\left[\frac{\partial v}{\partial z}\right]\!\right]$ (where v denotes the gas velocity along the z direction), thus making the result compatible with the Hadamard relation. A system of balance laws commonly presents several AWs which travel at different characteristic speeds. Here we will focus on the fastest wave, since it will be the only one to propagate in the unperturbed solution in the presence of multiple waves.

From (2) it is evident that the behavior of the scalar amplitude depends on its value at the initial instant. In particular, there exists a critical value $\mathcal{A}_{cr}$ such that if $\mathcal{A}_0/\mathcal{A}_{cr} > 1$, the amplitude $\mathcal{A}(t)$ diverges after a critical time t_{cr}, implying the transformation of the AW into a shock wave. Concerning this phenomenon, therefore, the study of the AWs can be considered as a study of the non-linear stability of the unperturbed solution. It is easy to prove that $\mathcal{A}_{cr} = -\lim_{t\to\infty} 1/g_2(t)$.

3 A simplified model of a gas bubble oscillating within a liquid

A gas bubble generated within a liquid is supposed to oscillate due to the presence of a periodic acoustic signal. For the sake of simplicity the form of such a bubble is assumed to be perfectly spherical, although several experimental data have shown that during its oscillations the bubble changes its shape, especially when violent shrinkages occur [3, 5]. The dynamics of bubble radius $R(t)$ is commonly described by an ordinary differential equation that accounts for the interaction between the gas bubble and the surrounding liquid [3, 5]. One of the most famous model for $R(t)$ is the Rayleigh-Plesset (RP) equation, which is valid under the assumption of incompressibility of the liquid:

$$R\ddot{R} + \frac{3}{2}\dot{R}^2 = \frac{1}{\rho_L}\Big(P_g - P_E + P_a(t)\Big) - \frac{4\eta\dot{R}}{\rho_L R} - \frac{2\varsigma}{\rho_L R} + \frac{R}{\rho_L c_L}\frac{d}{dt}(P_g + P_a), \qquad (5)$$

where ρ_L is the mass density of the liquid around the bubble, c_L its sound velocity, η represents the shear viscosity of the liquid, while ς denotes the surface tension. Moreover, P_E is the ambient pressure at equilibrium, $P_a(t) = P_a\cos(\omega t + \varphi_0)$ is the acoustic signal. Lastly, P_g is the gas pressure inside the bubble. In this respect we remind that the RP equation is deduced under the homobaric hypothesis, i.e. imposing that P_g is spatially homogeneous. Although in reality the gas pressure inside the bubble should not be uniform, due to several factors such as the acceleration of the bubble wall, it was verified that this effect is negligible, at least during the bubble expansion and the early stages of its shrinkage [1, 24]. It was verified that the homobaric hypothesis is not compatible with the physical conditions in the final stages of a violent contraction. However, the RP equation maintains its validity [4, 11]: this happens even in the presence of an AW, which generates an inhomogeneity in the bubble during its propagation [9].

To make (5) a stand-alone equation, integrable without coupling it with other equations (closure problem) it is necessary to express P_g as a function of $R(t)$. The simplest and most used technique fixes the dependence of the pressure on the bubble radius as $P_g = P_E\left(\frac{R_E}{R(t)}\right)^{3\kappa}$ where κ equals 1 in the isothermal case or is $\gamma = c_V/c_P$ (the ratio of the specific heats) under adiabatic conditions.

The emission of light from cavitation bubbles, with time resolution from microseconds to picoseconds, is a phenomenon called sonoluminescence, which is characterized by two different regimes: multi-bubble sonoluminescence (MBSL), when the light emission comes from a cloud of bubbles, and single-bubble sonoluminescence (SBSL), when the light emission occurs from a single bubble. Spectroscopic analyses of the emitted

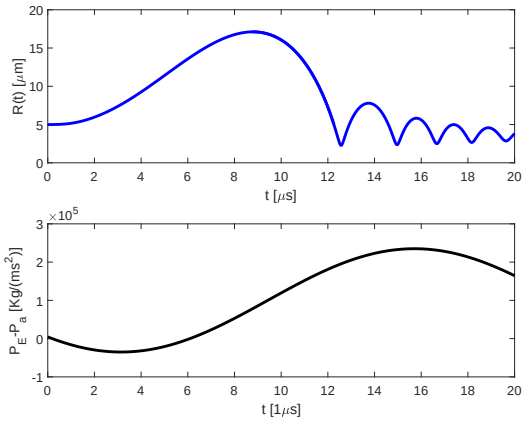

Fig. 1 Qualitative behaviour of bubble radius, $R(t)$, in the presence of a periodic acoustic signal, P_a.

light have revealed high temperatures and pressures associated with SL, especially for SBSL, when temperature up to 15000 K and pressures well over 10^3 atm are detected. However, the core temperature and the pressure of the collapsing bubble could be even higher, due to the presence of a region of optically opaque plasma which does not allow observation [25]. Bearing in mind the very rapid oscillation of the bubble, which occurs in time intervals of the order of microseconds, one can easily deduce the extraordinary conditions of temperature variation with heating and cooling rates of order of 10^{12} K/s [25]. A qualitative example of the non-linear oscillations of the bubble close to the SL regime is presented in Figure 1. The initial radius value is the equilibrium one R_E that corresponds to the absence of external sound signal and to the equilibrium of the bubble with the liquid. By activating the acoustic field $P_a(t)$ the bubble slowly increases its volume until it reaches the maximum radius R_M. A faster shrinkage follows the expansion, so that the $R(t)$ returns to R_E until it reaches the minimum value R_m (for particular violent contractions R_m could be close to the van der Waals hard core radius). Rebounds occur after this first contraction due to inertial effects. When the bubble contracts and its wall still presents negative acceleration ($R_M > R \geq R_E$) it is possible, as a first approximation, to neglect the viscous terms and the terms related to surface tension, as well as the effects produced by the internal pressure of the bubble, the acoustic signal and their variations [2, 3]. If the gas inside the bubble is supposed to be ideal, equation (5) is simplified as

$$\frac{1}{2}R^3\dot{R}^2 = \frac{P_E(R_M^3 - R^3)}{3\rho_L}. \tag{6}$$

4 The equations of the gas mixture inside the bubble

To model the gas mixture we refer to the theory of homogeneous mixtures introduced by Truesdell [26, 27] and developed by Mueller [28] in the context of rational thermodynamics, following the idea that it is possible to write the balance laws typical of a single gas for each component of the mixture. There is an immense literature on gas mixtures that employs both macroscopic approaches related to continuum theory and microscopic ones derived from kinetic theory [29–31].

In the present work we will refer to a MT model in which a different temperature is attributed to each species composing the mixture [29, 31–39]. This approach typical of plasma studies is capable of better representing non-equilibrium phenomena. We will also neglect the effects of thermal conductivity and viscosity, focusing on a mixture of Euler gases. In this way the resulting balance laws contain mass density, temperature and velocity of each mixture component as field variables.

In a spherical oscillating domain it is convenient to write the equations of the MT Euler mixture in spherical coordinates and assume a one-dimensional radial dependence of the fields. To further simplify the mathematical description of the phenomenon we also introduce a change of time-space variables $\{t, r\}$ (with r radial coordinate inside the bubble $r \in [0, R(t)]$), to the more comfortable $\{t', x\}$ if $t' = t$ and $x = r/R(t)$ with $x \in [0, 1]$, so as to work in a constant bounded domain. Referring to the works by Ruggeri and Simic on MT gas mixtures [31, 34, 35] the model system becomes

$$
\begin{aligned}
&\partial_t \rho_1 + \frac{v_1 - x\dot{R}}{R}\partial_x \rho_1 + \frac{\rho_1}{R}\partial_x v_1 = -2\frac{\rho_1 v_1}{Rx},\\
&\partial_t v_1 + \frac{k_B T_1}{m_1 \rho_1 R}\partial_x \rho_1 + \frac{v_1 - x\dot{R}}{R}\partial_x v_1 + \frac{k_B}{m_1 R}\partial_x T_1 = \frac{\mathcal{M}_1}{\rho_1},\\
&\partial_t T_1 + \frac{2T_1}{D_1 R}\partial_x v_1 + \frac{v_1 - x\dot{R}}{R}\partial_x T_1 = -\frac{4T_1 v_1}{D_1 R x} + \frac{2\mathcal{E}_1}{D_1 n_1},\\
&\partial_t \rho_2 + \frac{v_2 - x\dot{R}}{R}\partial_x \rho_2 + \frac{\rho_2}{R}\partial_x v_2 = -2\frac{\rho_2 v_2}{Rx},\\
&\partial_t v_2 + \frac{k_B T_2}{m_2 \rho_2 R}\partial_x \rho_2 + \frac{v_2 - x\dot{R}}{R}\partial_x v_2 + \frac{k_B}{m_2 R}\partial_x T_2 = -\frac{\mathcal{M}_1}{\rho_2},\\
&\partial_t T_2 + \frac{2T_2}{D_2 R}\partial_x v_2 + \frac{v_2 - x\dot{R}}{R}\partial_x T_2 = -\frac{4T_2 v_2}{D_2 R x} - \frac{2\mathcal{E}_1}{D_2 n_2},
\end{aligned}
\tag{7}
$$

where

$$
\begin{aligned}
&\mathcal{M}_1 = \psi_v\Big(\frac{u_2}{T_2} - \frac{u_1}{T_1}\Big) \qquad \mathcal{E}_1 = \psi_T\Big(\frac{1}{T_1} - \frac{1}{T_2}\Big),\\
&\psi_v = \frac{2m_1 m_2}{m_1 + m_2} T_a \Gamma_{12}, \quad \psi_T = \frac{3m_1 m_2}{(m_1 + m_2)^2} k_B T_a^2 \Gamma_{12},\\
&\psi_T = \frac{3m_1 m_2}{(m_1 + m_2)^2} T_a^2 \Gamma_{12}
\end{aligned}
\tag{8}
$$

and ρ_i, n_i, T_i and v_i denote mass and number density, temperature and radial component of the velocity of the i-species ($i = 1, 2$), while T_a is the average temperature. Γ_{12} represents the volumetric collisional frequency, while $u_i = v_i - \bar{v}$ is the diffusion velocity of the i-component and $\bar{v}$ the velocity of the mass centre defined below. Moreover, both gases are supposed to be ideal and polytropic so that the partial pressure p_i and the partial specific internal energy ε_i turn out to be

$$p_i = \frac{k_B}{m_i}\rho_i T_i, \quad \varepsilon_i = \frac{D_i k_B T_i}{2m_i}, \quad \text{with } \gamma_i = \frac{D_i + 2}{D_i} \tag{9}$$

if m_i is the molecular mass of gas i, while D_i are the corresponding molecular degrees of freedom and k_B the Boltzmann constant. The quantity associated to the entire gas mixture that could be measured in an experiment are the total mass density ρ (or number density n), the average temperature T_a and the mixture velocity (velocity of the mass centre) $\bar{v}$ that are defined as

$$\rho = \sum_{i=1}^{2} \rho_i, \quad n = \sum_{i=1}^{2} n_i, \quad \bar{v} = \frac{\rho_1 v_1 + \rho_2 v_2}{\rho}, \quad T_a = \frac{D_1 n_1 T_1 + D_2 n_2 T_2}{D_1 n_1 + D_2 n_2}. \tag{10}$$

The following characteristic polynomial is associated to the PDE set (7)

$$\begin{aligned} &\mathcal{P}(\lambda) = \mathcal{P}_1(\lambda)\mathcal{P}_2(\lambda) \quad \text{with } \mathcal{P}_i(\lambda) = (\lambda R - v_i + \dot{R}x)(a_i\lambda^2 + b_i\lambda + c_i) \quad \text{if } i = 1, 2 \\ &a_i = D_i m_i R^2, \quad b_i = -2D_i m_i R(v_i - \dot{R}x), \quad c_i = -(D_i + 2)k_B T_i + D_i m_i (v_i - \dot{R}x)^2, \end{aligned}$$

so that the corresponding characteristic speeds are easily determined as

$$\begin{aligned} \lambda_1 &= \frac{v_1 - \dot{R}x}{R}, \quad \lambda_{2,3} = \pm\frac{1}{R}\sqrt{\frac{(D_1 + 2)k_B T_1}{D_1 m_1}} + \frac{v_1 - \dot{R}x}{R}, \\ \lambda_4 &= \frac{v_2 - \dot{R}x}{R}, \quad \lambda_{5,6} = \pm\frac{1}{R}\sqrt{\frac{(D_2 + 2)k_B T_2}{D_2 m_2}} + \frac{v_2 - \dot{R}x}{R}. \end{aligned} \tag{11}$$

Hence, it can be concluded that the PDE system (7) is of hyperbolic type for any values of the field variables with physical meaning ($T_i > 0$). Moreover it is verified that if $v_1 = v_2$ and $m_1 \simeq m_2$, the highest characteristic speed is the one corresponding to the species with the smallest value of D_i, that is to say with the maximum ratio of specific heats γ_i.

A mixture of Euler gases within a bubble has often been described as a single perfect gas (SG) with mass density ρ, temperature T e velocity v [7, 8]. In such a case the gas will be attributed a molecular mass equal to $\bar{m}$ and a number of molecular degrees of freedom equal to $\bar{D}$ given by

$$\bar{m} = \frac{n_1 m_1 + n_2 m_2}{n}, \quad \bar{D} = \frac{n_1 D_1 + n_2 D_2}{n} \tag{12}$$

so that the gas equations reduce to Euler conservation of mass, momentum and energy:

$$\begin{aligned}
&\partial_t \rho + \frac{v - x\dot{R}}{R}\partial_x \rho + \frac{\rho}{R}\partial_x v = -2\frac{\rho v}{Rx}, \\
&\partial_t v + \frac{k_B T}{\bar{m}\rho R}\partial_x \rho + \frac{v - x\dot{R}}{R}\partial_x v + \frac{k_B}{\bar{m}R}\partial_x T = 0, \\
&\partial_t T + \frac{2T}{\bar{D}R}\partial_x v + \frac{v - x\dot{R}}{R}\partial_x T = -\frac{4Tv}{\bar{D}Rx}
\end{aligned} \tag{13}$$

to which the characteristic speeds $\lambda^{(S)}$ correspond

$$\lambda_1^{(S)} = \frac{v - \dot{R}x}{R}, \quad \lambda_{2,3}^{(S)} = \pm\frac{1}{R}\sqrt{\frac{(\bar{D}+2)k_B T}{\bar{D}\bar{m}}} + \frac{v - \dot{R}x}{R}. \tag{14}$$

In the following sections we will refer to this second hyperbolic dissipation-free model as a term of comparison.

5 Acceleration waves propagating in an oscillating bubble filled with a binary gas mixture

5.1 Preliminary assumptions

The oscillating bubble wall could act like a piston on the gas, generating an incoming spherical AW. To simplify the study of such a wave, and in particular the determination of the coefficients (4) and the behavior of the scalar amplitude (2), some reasonable approximations are introduced here.

- The bubble radius is assumed to depend linearly on time:

$$R(t) = R_0(1 + \mu t), \tag{15}$$

  where R_0 is the initial bubble radius and $\dot{R} = R_0\mu$ can be evaluated referring to (6), during the shrinkage. This linearity of $R(t)$ holds true only for small time intervals, consistent with the short time taken by AW to travel from the wall to centre of the bubble.
- The unperturbed radial velocities of the components are equal and linear in x:

$$v_1 = v_2 = x\dot{R}. \tag{16}$$

- The relaxation terms (8) are linearized in the non-equlibrium variables as well, referring to [29, 31] they can be reduced to ($\sigma_{12} = (\sigma_1 + \sigma_2)/2$ is the average

molecular diameter and $r_m = m_1/m_2$ the ratio of the molecular masses)

$$\begin{aligned}
&\frac{\mathcal{M}_1}{\rho_1} \simeq \frac{v_2 - v_1}{\tau_v}, \qquad \frac{2\mathcal{E}_1}{n_1} \simeq \frac{T_2 - T_1}{\tau_T} \\
&\frac{1}{\tau_v} = \frac{4\sqrt{2\pi}}{\sqrt{1 + r_m^{-1}}} \sqrt{k_B T_0 m_2} n_{20} \sigma_{12}^2, \quad \frac{1}{\tau_T} = \frac{12\sqrt{2\pi}}{r_m (1 + r_m^{-1})^{3/2}} \sqrt{\frac{k_B T_0}{m_2}} n_{20} \sigma_{12}^2. \\
&\frac{1}{\tau_v} = \frac{4\sqrt{2\pi}}{r_m \sqrt{1 + r_m^{-1}}} \sqrt{\frac{k_B T_0}{m_2}} n_{20} \sigma_{12}^2
\end{aligned} \tag{17}$$

Hence, the relaxation times τ_v and τ_T are modelled as constant quantities, determined at established initial values of the average temperature T_0 and the number densities.

These simplifying assumptions allow a semi-analytical description of the AW, implying the adiabaticity and the space homogeneity of mass density, temperature and pressure.

In order to determine the unperturbed solution, we prescribe the initial values of equilibrium temperature of the two species T_{i0} and of the corresponding mass densities ρ_{i0} $(i = 1, 2)$. For the sake of simplicity, here we always assume that component 1 of the mixture presents a number of degrees of freedom $D_1 > D_2$ (hence $\gamma_1 < \gamma_2$) and that the masses of the two species are such that the maximum absolute values of the characteristic speed is $\lambda_5 = |\lambda_6|$ ($r_m > r_\gamma$ if $r_\gamma = \gamma_1/\gamma_2$). Since we are studying the AWs propagating with a negative velocity, from now on we will focus our attention on the wave corresponding to λ_6.

5.2 Unperturbed solution

Under the previous hypotheses it is possible to easily derive the equations for the unperturbed solution $\mathbf{u}_u = (\rho_{1u}, v_{1u}, T_{1u}, \rho_{2u}, v_{2u}, T_{2u})$:

$$\begin{aligned}
&\rho_{1u} = \rho_{10} \frac{R_0^3}{R^3}, \quad \rho_{2u} = \rho_{20} \frac{R_0^3}{R^3} \\
&v_{1u} = v_{2u} = x\dot{R} = x R_0 \mu, \\
&\partial_t T_{1u} = -\frac{6 T_{1u} \dot{R}}{D_1 R} + \frac{T_{2u} - T_{1u}}{D_1 \tau_T}, \\
&\partial_t T_{2u} = -\frac{6 T_{2u} \dot{R}}{D_2 R} - \frac{(T_{2u} - T_{1u}) r_n}{D_2 \tau_T},
\end{aligned} \tag{18}$$

if $n_{i0} = \rho_{i0}/m_i$ denote the initial value of the number of the i-component, so that $r_n = n_{10}/n_{20}$ represents the ratio of the concentrations of the two gases. It can be easily verified that if $\dot{R} = R_0 \mu \neq 0$ the solution $T_{1u} = T_{2u}$ is impossible if the two mixture components present different specific heats (and so different D_i). In Figs. 2-4 we show the qualitative behaviour of T_{1u} and T_{2u} during the propagation of the AW towards the bubble centre if a linear shrinkage of the bubble is taken into account. Such a propagation occurs immediately after an isothermal transformation, so that $T_{10} = T_{20} = T_0 = 300\text{K}$ are the initial values of the temperature used to integrate

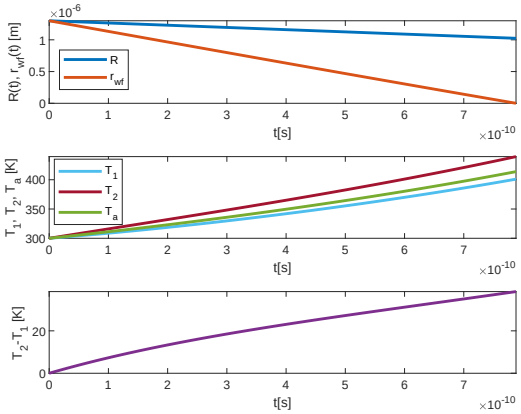

Fig. 2 The case of a bubble of radius $R(t)$ (with equilibrium radius $R_E = 1\mu$m) filled by a gas mixture of CO_2 and He ($r_m = 11$) with the same number density ($r_n = 1$). The figure shows the behaviour of the AW front ($r_{wf}(t)$) in (t, r) time-space variables during its travel from the bubble wall to the centre. Moreover one can find the plot of the average temperature of the gas mixture and of the corresponding temperatures of the two species, besides their difference.

(18). The role of the parameters R_E, r_n and r_m is studied. We fix $D_2 = 3$ (monatomic gas) and $D_1 = 6$; $R_M = 10R_E$ and the initial radius $R_0 = 7.7R_E$ in all the figures. In addition, $r_m = 11$ (a mixture of carbon dioxide and helium) in Figs. 2 and 4, while $r_m = 1.1$ (a mixture of carbon dioxide and argon) in Fig. 3. The ratio r_n is prescribed to be 3 in Fig. 4 on the top and to be 1 in the remaining cases. Finally R_E is equal to 1μm in all the figures except Fig. 4 on the bottom, where it is assumed to be 10μm. The figures show a rapid growth in temperature compatible with what was observed experimentally for SL regime, as already described in Sec. 3 [25]. The temperature difference $T_2 - T_1$ increases as the bubble radius decreases, since in smaller bubbles the gases are further from equilibrium. Differences in number densities and in molecular masses could exacerbate the phenomenon, as well.

5.3 Calculation of Bernoulli coefficients

Referring to the fastest AW with unperturbed characteristic speed

$$\lambda_u = -\frac{1}{R}\sqrt{\frac{(D_2+2)k_B T_{2u}}{D_2 m_2}} \tag{19}$$

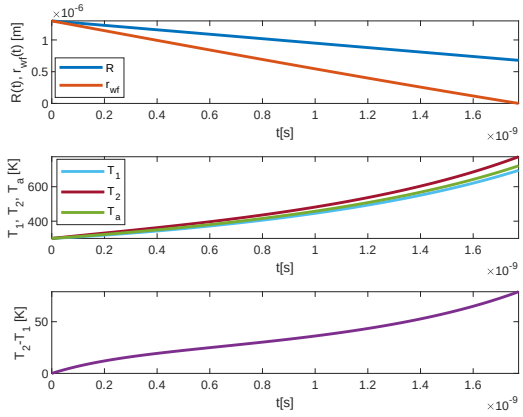

Fig. 3 The case of a bubble of radius $R(t)$ (with equilibrium radius $R_E = 1\mu$m) filled by a gas mixture of CO_2 and Ar ($r_m = 1.1$) with $r_n = 1$. The figure shows the behaviour of the AW front ($r_{wf}(t)$) during its travel from the bubble wall to the centre. Moreover one can find the plot of the average temperature of the gas mixture and of the corresponding temperatures of the two species, besides their difference.

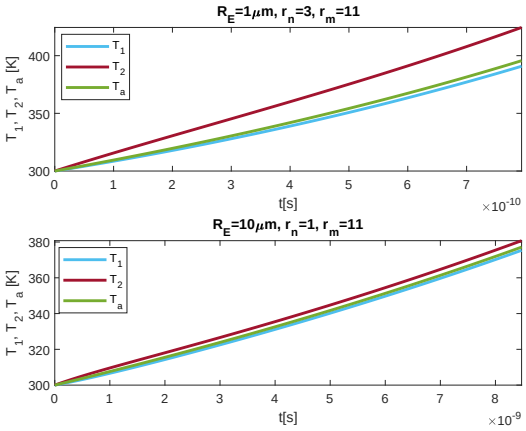

Fig. 4 The case of a bubble with equilibrium radius $R_E = 1\mu$m on the top and $R_E = 10\mu$m (on the bottom) filled by a gas mixture of CO_2 and He ($r_m = 11$) with $r_n = 3$ on the top and $r_n = 1$ on the bottom. The figure shows the behaviour of the average temperature of the gas mixture and of the corresponding temperatures of the two species.

and corresponding right and left unperturbed eigenvectors

$$\mathbf{r}_u = \left(0, 0, 0, -\frac{\rho_{2u}}{\lambda_u^2 R}, -\frac{1}{\lambda_u}, -\frac{2T_{2u}}{D_2 \lambda_u^2 R}\right), \quad \mathbf{l}_u = \left(0, 0, 0, \frac{k_B l_5 T_{2u}}{\lambda_u m_2 \rho_{2u} R}, l_5, \frac{k_B l_5}{\lambda_u m_2 R}\right), \tag{20}$$

with $l_5 = -D_2 \lambda_u^3 m_2 R^2 (D_2 \lambda_u^2 m_2 R^2 + (D_2 + 2) k_B T_{2u})^{-1}$. The equation of the corresponding wave front in (x, t) variables is formally written as

$$x_{wf}(t) = 1 + \int_0^t \lambda_u(s) ds \tag{21}$$

and can be determined numerically once equations (18) are solved. The corresponding Bernoulli's coefficients are obtained from (4)

$$\begin{aligned}
a &= -\frac{D_2 + 1}{D_2 \lambda_u R}, \\
b &= \frac{3(D_2+1)\dot{R}}{2D_2 R} + \frac{\lambda_u}{x_{wf}} + \frac{-(D_2-2)T_{1u} + (D_2+2)T_{2u}}{2D_2(D_2+2)k_B n_{20} T_{2u} \tau_T} + \frac{1}{2\tau_v m_2 n_{20}}. \\
b &= \frac{3(D_2+1)\dot{R}}{2D_2 R} + \frac{\lambda_u}{x_{wf}} + \frac{-(D_2-2)T_{1u} + (D_2+2)T_{2u}}{4D_2(D_2+2) r_n^{-1} T_{2u} \tau_T} + \frac{1}{2\tau_v r_m^{-1} r_n^{-1}}. \\
b &= \frac{3(D_2+1)\dot{R}}{2D_2 R} + \frac{\lambda_u}{x_{wf}} + \frac{-(D_2-2)T_{1u} + (D_2+2)T_{2u}}{4D_2(D_2+2) r_n^{-1} T_{2u} \tau_T} + \frac{1}{2\tau_v r_m^{-1} r_n^{-1}}.
\end{aligned} \tag{22}$$

We observe that both coefficients depend on parameters and unperturbed temperature of component 2 (the one corresponding to the fastest AW). The coefficient b is also function of the unperturbed temperature of component 1, or, which is the same, of the unperturbed average temperature. This fact is related to the non-stationary structure of the unperturbed solution (18).

5.4 Numerical analysis of some physical cases

In 1978 it was first demonstrated [14] that spherical AWs travelling towards the centre exhibit a singularity that is peculiar to this geometry. This fact implies the formation of shock waves for any initial negative scalar amplitude $\mathcal{A}_0$ [6, 9, 14]. On the other hand, it is possible to verify that this phenomenon occurs in a very small neighbourhood around the centre of the sphere, but a continuum mechanics theory such as the one we are using is unable to predict phenomena that occur on spatial scales smaller than the kinetic diameter ($\mathfrak{d}$) of a molecule. What should happen is a reflection of the AW before reaching such a neighbourhood. For this reason here we will refer to the concept of special critical amplitude which corresponds to the greatest negative value of $\mathcal{A}_0$ for which shock formation is observed before the wavefront reaches the distance $\mathfrak{d}$ from the centre. From (2), it is easily demonstrated that

$$\exists t^* \in R^+ : \quad R(t^*) x_{wf}(t^*) = \mathfrak{d} \qquad \text{and} \quad \mathcal{A}_{cr}^* = -1/g_2(t^*).$$

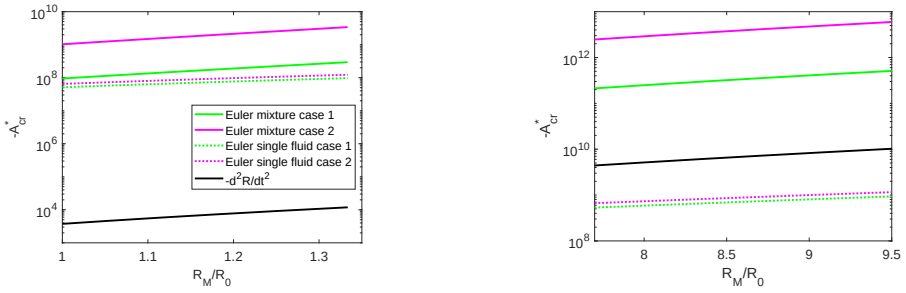

Fig. 5 $-\mathcal{A}^*_{cr}$ values for the MT (continuous line) and the SG (dotted line) models, compared with $-\ddot{R}$. On the left the case $R_0 \simeq R_M$, on the right $R_0 \simeq R_E$ (close to the sonoluminescence zone). Case 1 a mixture of CO_2 and Ar; Case 2: a mixture composed by CO_2 and He.

In the last figure we present an example of calculation of $\mathcal{A}^*_{cr}$ ($\mathfrak{d} \simeq 2 \times 10^{-10} m$) for two different gas mixtures composed by CO_2 and Ar (case 1) and CO_2 and He (case 2), prescribing $r_n = 3$, $R_E = 10\mu$m, $\sigma_{12} \simeq 3 \times 10^{-10}$m, $D_1 = 6$, $D_2 = 3$. The values are evaluated during the shrinkage in two different phases: $R_0 \simeq R_M$ (on the left) and $R_0 \simeq R_E$ (on the right). Moreover, the calculations are performed taking into account two different models: the MT Euler one (solid line) and the SG Euler equations (dotted line). The system (7) requires numerical integrations in order to determine the explicit expression of the wave front, the Bernoulli's coefficients and the function $g_2(t)$, while for the SG Euler balance laws (13) we refer to previous analytical results in [9]. Shock formation is assumed to be possible if the acceleration of the bubble wall $\ddot{R}$ (black line) is negative and comparable to the value of $\mathcal{A}^*_{cr}$. From Fig. 5 it is evident that this case only occurs for the SG model and when $R_0 \simeq R_E$, since the special critical amplitude usually differs by several orders of magnitude from the wall acceleration (estimated through (6) approximation). One can conclude that the dissipation gives rise to a highly stabilizing effect and tends to inhibit the onset of shocks. This phenomenon is even more evident for small bubbles, where the wave propagation times are comparable with the relaxation times of model (7) with (17).

6 Conclusions

What elements are indispensable for modelling the gas inside a bubble that oscillates periodically in a liquid? To contribute to the complex answer to this question, we have studied the case of a MT binary mixture of Euler gases. Through the AWs instrument it is possible to demonstrate that the dissipation linked to the temperature difference plays an important role, among other things by inhibiting the shock formation. The dynamics of the gas and, therefore, also that of the bubble appear to be the result of the competition between the dissipations, which tend to bring the system back to an equilibrium state, and the periodic oscillation, which incessantly restores the non-equilibrium conditions. The topic will be the subject of further study in a forthcoming work.

Acknowledgments. Dedicated to Giuseppe Mulone with great esteem and friendship. This work was carried out in the framework of the activities of Gruppo Nazionale di Fisica Matematica GNFM-INdAM and was supported in part (F.B.) by the Italian research Project PRIN 2017 No. 2017YBKNCE "Multiscale phenomena in Continuum Mechanics: singular limits, off-equilibrium and transitions".

Declarations

Conflict of interest: The authors declare that they have no conflict of interest.

References

[1] Prosperetti, A.: The thermal behaviour of oscillating gas bubbles. J. Fluid Mech. **222**, 587–616 (1991)

[2] Loefstedt, R., Barber, B.P., Putterman, S.J.: Toward a hydrodynamic theory of sonoluminescence. Phys. Fluids A **5**, 2911–2928 (1993)

[3] Barber, B., Hiller, R., Loefstedt, R., Putterman, S.J., Weninger, K.R.: Defining the unknowns of sonoluminescence. Physics Reports **281**, 65–143 (1997)

[4] Brenner, M.P., Hilgenfeldt, S., Lohse, D.: Single-bubble sonoluminescence. Rev. Mod. Phys. **74**, 425–484 (2002)

[5] Lauterborn, W., Kurz, T.: Physics of bubble oscillations. Rep. Prog. Phys. **73**, 106501 (2010)

[6] Greenspan, H.P., Nadim, A.: On sonoluminescence of an oscillating gas bubble. Phys. Fluids A **5**, 1065–1067 (1993)

[7] Wu, C.C., Roberts, P.H.: Shock-wave propagation in a sonoluminescencing gas bubble. Phys. Rev.Lett. **70**, 3424–3427 (1993)

[8] Wu, C.C., Roberts, P.H.: A model of sonoluminescence. Proc. Royal Soc. London A **445**, 323–349 (1994)

[9] Brini, F., Seccia, L.: Acceleration waves and oscillating gas bubbles modelled by rational extended thermodynamics. Proc. Royal Soc. A **478**, 20220246 (2022)

[10] Vuong, V.Q., Szeri, A.J.: Sonoluminescence and diffusive transport. Phys. Fluids **8**, 2354–2364 (1996)

[11] Lin, H., Storey, B.D., Szeri, A.J.: Inertially driven inhomogeneities in violently collapsing bubbles: the validity of the rayleigh-plesset equation. J. Fluid Mech. **452**, 145–162 (2002)

[12] Boillat, G.: La Propagation des Ondes. Gauthier-Villars, Paris, France (1965)

[13] Bowen, R.M., Doria, M.L.: Effect of diffusion on the growth and decay of acceleration waves in gases. J. Acoust. Soc. America **53**, 75–82 (1973)

[14] Lindsay, K.A., Straughan, B.: Acceleration waves and second sound in a perfect fluid. Arch. Ration. Mech. Anal. **68**, 54–87 (1978)

[15] Boillat, G., Ruggeri, T.: On the evolution of weak discontinuities for hyperbolic quasi-linear systems. Wave Motion **1**, 149–152 (1979)

[16] Ruggeri, T.: Stability and discontinuity waves for symmetric hyperbolic systems. In: Jeffrey, A. (ed.) Nonlinear Wave Motion, pp. 148–161. Longman, New York (1989)

[17] Muracchini, A., Ruggeri, T.: Acceleration waves, shock formation and stability in a gravitating atmosphere. Space Sci. **153**, 127–142 (1989)

[18] Ruggeri, T., Seccia, L.: Hyperbolicity and wave propagation in extended thermodynamics. Meccanica **24**, 127–138 (1989)

[19] Muracchini, A., Seccia, L.: Thermo-acceleration waves and shock formation in extended thermodynamics of gravitational gases. Cont. Mech. Thermodyn. **1**, 227–237 (1989)

[20] Jordan, P.M., Straughan, B.: Acoustic acceleration waves in homentropic green and naghdib gases. Proc. R. Soc. A **462**, 3601–3611 (2006)

[21] Barbera, E., Valenti, G.: Kawashima condition and acceleration waves for binary non reacting mixtures. Acta Mech. **187**, 203–217 (2006)

[22] Brini, F., Seccia, L.: Acceleration waves in rational extended thermodynamics of rarefied monatomic gases. Fluids **5**(139) (2020)

[23] Rester, B., Lambers, J.V., Jordan, P.M.: Acoustic singular surfaces in an exponential class of inhomogeneous gases: A new numerical approach based on krylov subspace spectral methodologies. Int. J. Non-lin. Mech. **156**, 104506 (2023)

[24] Man, Y., Trujillo, F.J.: A new pressure formulation for gas-compressibility dampening in bubble dynamics models. Ultrasonics Sonochem. **32**, 247–257 (2016)

[25] Suslick, K.S., Flannigan, D.J.: Inside a collapsing bubble: sonoluminescence and the conditions during cavitation. Annu. Rev. Phys. Chem. **59**, 659–683 (2008)

[26] Trusdell, C.: Sulle basi della termodinamica i. Rend. Sc. Fis. Mat. Nat. **22**, 33–38 (1957)

[27] Trusdell, C.: Sulle basi della termodinamica ii. Rend. Sc. Fis. Mat. Nat. **22**, 158–166 (1957)

[28] Mueller, I.: A thermodynamic theory of mixtures of fluids. Arch. Ration. Mech. Anal. **28**, 1–39 (1968)

[29] Chapman, S., Cowling, T.G.: The Mathematical Theory of Non-uniform Gases. Cambridge University Press, Cambridge (1970)

[30] Mueller, I., Ruggeri, T.: Rational Extended Thermodynamics. Springer, New York (1998)

[31] Ruggeri, T., Sugiyama, M.: Classical and Relativistic Rational Extended Thermodynamics of Gases. Springer, Cham (2021)

[32] Kanappan, D., Bose, T.K.: Transport properties of a two-temperature argon plasma. Physics of Fluids **20**, 1668–1673 (1977)

[33] Bose, T.K., Seeniraj, R.V.: Two-temperature noble gas plasmas. i. thermodynamics and transport coefficients. J. Indian Inst. Sci. **64**, 181–193 (1983)

[34] Ruggeri, T., Simic, S.: On the hyperbolic system of a mixture of eulerian fluids: a comparison between single and multi-temperature models. Math. Meth. Appl. Sci. **30**, 827–849 (2007)

[35] Ruggeri, T., Simic, S.: Average temperature and maxwellian iteration in multi-temperature mixtures of fluids. Phys. Rev. E **80**, 026317 (2009)

[36] Madjarevic, D., Ruggeri, T., Simic, S.: Shock structure and temperature overshoot in macroscopic multi-temperature model of mixtures. Phys. Fluid. **26**, 106102 (2014)

[37] Bisi, M., Martalò, G., Spiga, G.: Multi-temperature euler hydrodynamics for a reacting gas from a kinetic approach to rarefied mixtures with resonant collisions. EPL **95**, 55002 (2011)

[38] Bisi, M., Martalò, G., Spiga, G.: Multi-temperature fluid-dynamic model equations from kinetic theory in a reactive gas: The steady shock problem. Comp. Math. Appl. **66**, 1403–1417 (2013)

[39] Ruggeri, T., Taniguchi, S.: A complete classification of sub-shocks in the shock structure of a binary mixture of eulerian gases with different degrees of freedom. Phys. Fluid. **34**, 066116 (2022)